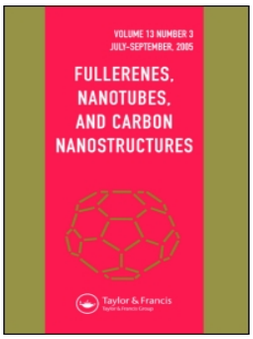

Fullerenes, Nanotubes and Carbon Nanostructures

ISSN: 1536-383X (Print) 1536-4046 (Online) Journal homepage: www.tandfonline.com/journals/lfnn20

Sn/SnO_2/Mwcnt composite anode and electrochemical impedance spectroscopy studies for Li-ion batteries

Mirac Alaf, Ubeyd Tocoglu, Fuat Kayis & Hatem Akbulut

To cite this article: Mirac Alaf, Ubeyd Tocoglu, Fuat Kayis & Hatem Akbulut (2016) Sn/SnO_2/Mwcnt composite anode and electrochemical impedance spectroscopy studies for Li-ion batteries, Fullerenes, Nanotubes and Carbon Nanostructures, 24:10, 630-634, DOI: 10.1080/1536383X.2016.1221403

To link to this article: https://doi.org/10.1080/1536383X.2016.1221403

Published online: 15 Aug 2016.

FULLERENES, NANOTUBES AND CARBON NANOSTRUCTURES
2016, VOL. 24, NO. 10, 630–634
http://dx.doi.org/10.1080/1536383X.2016.1221403

Taylor & Francis
Taylor & Francis Group

Sn/SnO_2/Mwcnt composite anode and electrochemical impedance spectroscopy studies for Li-ion batteries

Mirac Alaf[a], Ubeyd Tocoglu[b], Fuat Kayis[b], and Hatem Akbulut[b]

[a]Department of Metallurgy and Materials Engineering, Engineering Faculty, Bilecik Seyh Edebali University, Gulumbe Campus, Bilecik, Turkey;
[b]Department of Metallurgy and Materials Engineering, Engineering Faculty, Sakarya University, Esentepe Campus, Sakarya, Turkey

ABSTRACT

Tin/tinoxide/multi-walled carbon nanotube (Sn/SnO_2/MWCNT) core-shell structure nanocomposite anode is produced by thermal evaporation and subsequent plasma oxidation with using MWCNT buckypaper. Metallic tin is evaporated onto free-standing and flexible MWCNT buckypaper having controlled porosity and subsequent RF plasma oxidized in Ar:O_2(1:1) gas mixture. X-ray diffraction and scanning electron microscopy are used to determine the structure and morphology of the obtained nanocomposite. The electrochemical characteristics of the nanocomposite anode are examined by using electrochemical impedance spectroscopy and galvanostatic charge–discharge experiments. Family of Nyquist plots during first discharge process are obtained and studied at different voltage values.

ARTICLE HISTORY
Received 29 July 2016
Accepted 3 August 2016

KEYWORDS
tinoxide; electrochemical impedance spectroscopy; Li-ion battery; carbon nanotube

1. Introduction

Lithium-ion (Li-ion) batteries have high energy density and high-power density, and this combination may allow their use in various electric grid applications, including portable electronics, power tools, hybrid/full electric vehicles, and improving the quality of energy harvested from wind, solar, geothermal, and other renewable sources. Therefore, Li-ion batteries have received significant academic and industry interest in recent years (1). There also has been more interest recently in flexible and bendable energy storage devices, especially in the field of Li-ion batteries. Recent advanced technology in various types of soft portable electronic equipment, such as roll-up displays, wearable devices, and implanted medical devices, requires development of flexible batteries as their power sources (2).

Graphite has been employed as an anode material in Li-ion batteries. However, graphite has an inherent limitation with a theoretical gravimetric capacity at 372 mAh g^{-1} (3). For the purpose of improving the energy density of batteries, scientists have made great efforts to explore alternative anode materials with higher capacity, such as Si (4), Sn (5), Zn (6), transition-metal oxides (6) and their alloys (7), and composites (8). Among these potential anode materials, SnO_2-based materials have become one of the promising candidates, as SnO_2 has high theoretical capacity, the environmental friendliness of its raw material processing and low cost (9). However, SnO_2 could generate huge volume expansion/shrinkage (up to 259%) during the processes of charge and discharge lead to electrode pulverization; consequently, result in a large irreversible capacity loss and poor cycling stability (10). Different strategies have been proposed to overcome this problem of tin-based electrodes. One effective way is to disperse tin-based materials in a carbon matrix or encapsulate them with carbon to accommodate the strain of volume change during the alloying and dealloying processes of Li-Sn (11).

Electrochemical impedance spectroscopy (EIS) is one of the most universal and powerful electroanalytical techniques for fine characterization of kinetic and transport processes occurring in electrodes (12). The EIS method is based on the registration of frequency dependences (spectra, complex plane plots) of the electrochemical cell impedance and their further interpretation using the technique of equivalent circuits (ECs) (13).

In this study, Sn/SnO_2 double phase nanocomposite structure was deposited onto MWCNT buckypaper having controlled pores by a two-step fabrication method of thermal evaporation and subsequent plasma oxidation. It was aimed to penetrate Sn/SnO_2 structure the buckypaper pores which cannot only accommodate the large-volume changes that accompany the charge/discharge, but also provide good contact for the tin-based materials. Structural and electrochemical characterization of flexible and free-standing Sn/SnO_2/MWCNT nanocomposite anode were introduced. Family of Nyquist plots during first discharge process were obtained and studied at different voltage values.

2. Experimental details

Production of Sn/SnO_2/MWCNT composite anode is a multiple-stage process that includes preparing MWCNT

CONTACT Mirac Alaf mirac.alaf@bilecik.edu.tr Department of Metallurgy and Materials Engineering, Engineering Faculty, Bilecik Seyh Edebali University, Gulumbe Campus, 11210, Bilecik, Turkey.

Color versions of one or more of the figures in the article can be found online at www.tandfonline.com/lfnn.

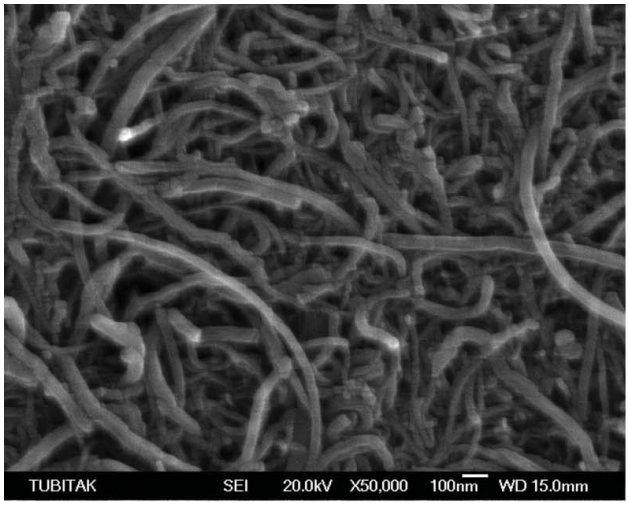

(a)

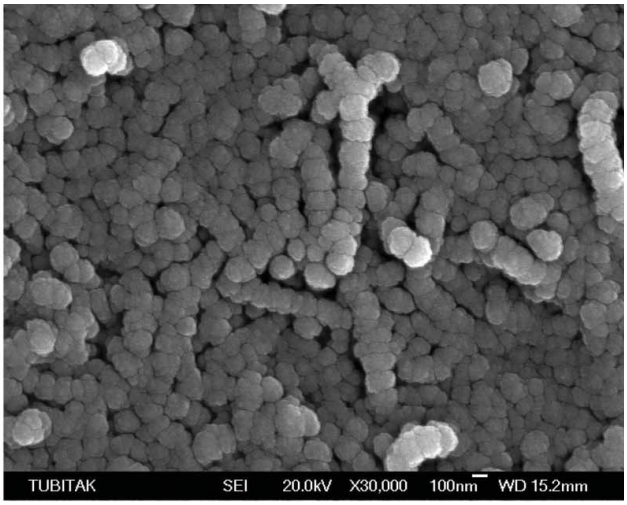

(b)

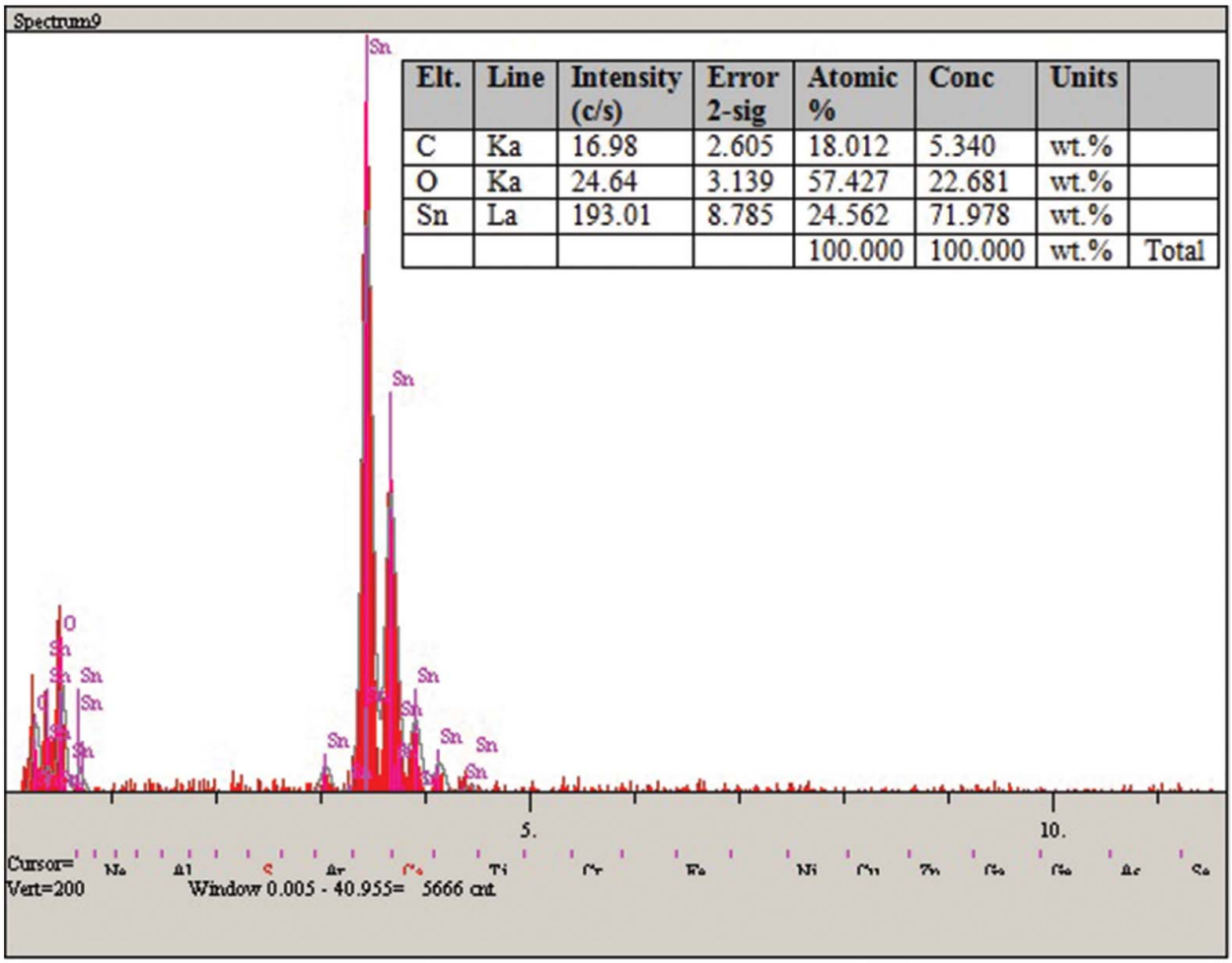

Elt.	Line	Intensity (c/s)	Error 2-sig	Atomic %	Conc	Units	
C	Ka	16.98	2.605	18.012	5.340	wt.%	
O	Ka	24.64	3.139	57.427	22.681	wt.%	
Sn	La	193.01	8.785	24.562	71.978	wt.%	
				100.000	100.000	wt.%	Total

(c)

Figure 1. (a) SEM image of CNT buckypaper, (b) and (c) SEM image and EDS spectrum of Sn/SnO_2/MWCNT composite from surface.

buckypaper, thermal evaporation of Sn onto this buckypaper, and plasma oxidation of this buckypaper. Before production of MWCNT buckypaper having controlled porosity with vacuum filtration technique, purification, and chemical oxidation of MWCNTs (from Arry Nano Germany) was carried out with different oxidation agents (14). In the second step, the buckypaper was attached the multifunctional physical vapor deposition (PVD) system as a substrate. Thermal evaporation of high-purity

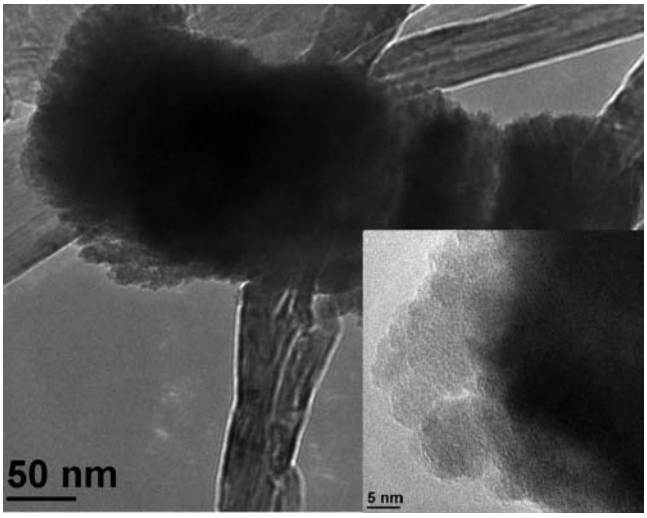

Figure 2. TEM image of Sn/SnO_2/MWCNT composite anode.

metallic tin (99.999%) under 1 Pa Ar atmosphere was carried out onto the buckypaper. Then, to obtain SnO_2, RF plasma oxidation was utilized under Ar:O_2 1:1 atmosphere (15).

An X-ray diffraction (XRD) (Rigaku D/MAX 2000) with Cu-Ka radiation has been used to determine the composition and structure of the nanocomposite. Transmission electron microscopy (TEM, Tecnai G2 F20 S-TWIN) and field emission gun scanning electron microscopy (FEG-SEM, JEOL 6335F) were used for examine surface morphologies. TEM samples of the anode paper were prepared by removing a small piece from the paper and mounting it on a folding copper mesh oyster grid. Coin-type (CR2016) test cells were assembled in an argon-filled glove box and the details of the CR2016 button-type cell assembling can be found in our previous work (15). The cells were cyclically tested on a MTI BST8-MA Battery Analyzer using constant current density (0.5 C) over a voltage range of 0.2–3 V. EIS measurements were carried out on the samples using a sine wave of 10 mV amplitude over a frequency range of 100 kHz–0.01 Hz using Gamry Instrument Version 5.67. The mass of active material in the Sn/SnO_2/MWCNT nanocomposite electrode was calculated as:

$$M_{\text{active}} = M_{\text{Sn}/\text{SnO}_2} + M_C \quad (1)$$

Where $M\frac{\text{Sn}}{\text{SnO}_2}$ was the Sn/SnO_2 coating's mass and M_C was mass of the Sn/SnO_2-coated carbon nanotubes participating in the lithiation/delithiation process. Depth of Sn/SnO_2-coated carbon nanotubes were measured with the aid of dot-map EDS analyzes and mass of CNT was calculated (16).

3. Results and discussions

MWCNT buckypaper was produced as flexible, smooth, and crack free by vacuum filtration technique from purified and chemically oxidized MWCNTs. After vacuum filtration, buckypaper was easily peeled off polyvinylidene difluoride (PVDF) membrane (has 220-nm pore size) and dried at

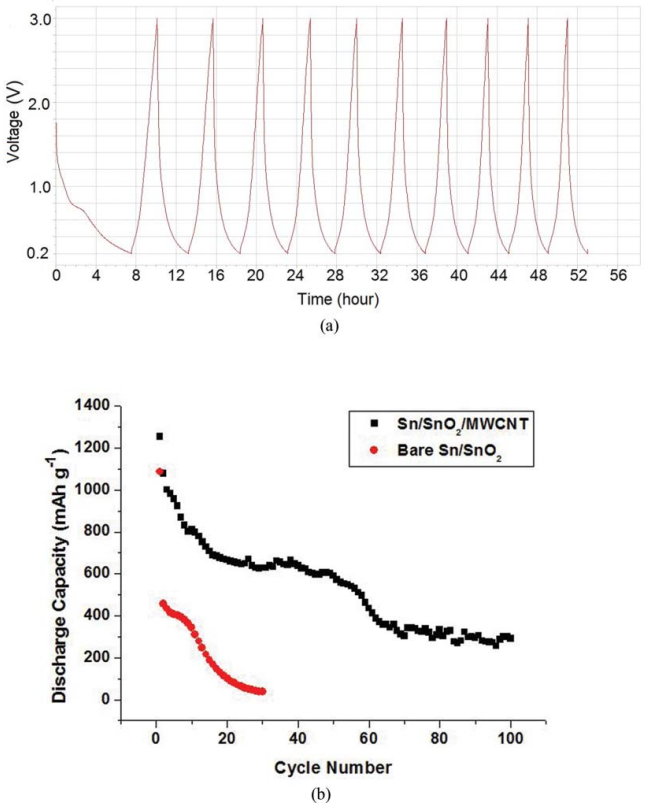

Figure 3. (a) Graph of voltage (V)-time (hour) Sn/SnO_2/MWCNT anode and (b) discharge capacities the anodes.

60°C. After thermal evaporation of high-purity tin onto MWCNT buckypaper and plasma oxidation,

Sn/SnO_2/MWCNT composite anode was successfully produced. XRD results of the composite were showed in our previous work (15). Figure 1a shows SEM image of CNT buckypaper without Sn/SnO_2. Figure 1b presents SEM image of Sn/SnO_2/MWCNT composite from surface and EDS spectrum. As can be seen from the Figure 1b Sn-based phases were deposited around the MWCNTs forming a core-shell structure. In Figure 1c, EDS spectrum shows atomic percent of Sn, O, and C elements. The results demonstrate proper percent values with XRD results.

SnO_2/Sn/MWCNT nanocomposite was further analyzed by TEM in order to confirm the presence of Sn and SnO_2 nanoparticles onto MWCNT surfaces and fine particles. TEM sample was prepared by removing a small piece of the anode paper and mounting it onto a folding copper mesh oyster grid. Figure 2 presents image of uncoated MWCNTs and coated MWCNT with Sn/SnO_2. The figure implies that the crystal size of the deposited Sn/SnO_2 is very fine and approximately 5 to 10 nm. Gao et al. (17) presented CNTs coated with thick layers of SnO_2 TEM images similar to our results.

Sn/SnO_2/MWCNT anode paper was electrochemically investigated in CR2016 Li-ion button cell. For comparing Sn/SnO_2, structure was deposited onto stainless steel under the same conditions. Figure 3a shows graph of voltage (V)-time (hour) for Sn/SnO_2/MWCNT anode. Figure 3b presents discharge capacities per gram versus cycle number for Sn/SnO_2/MWCNT anode and bare Sn/SnO_2 anode. The

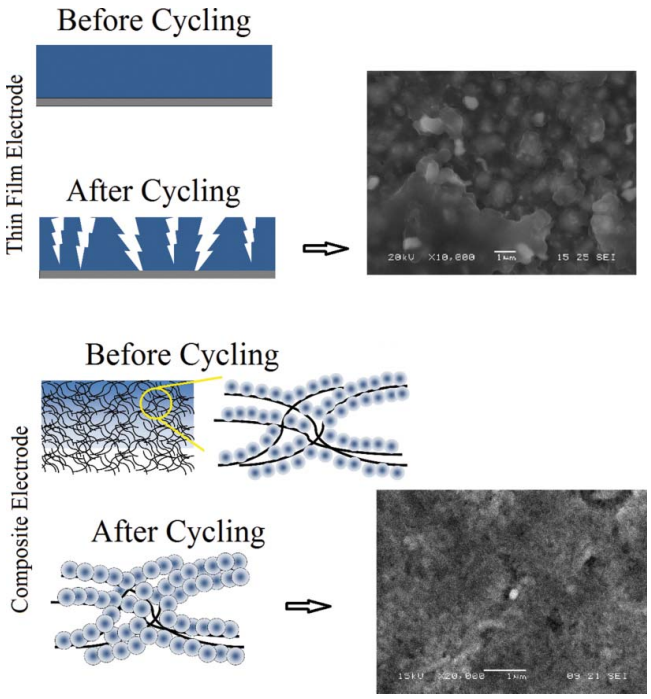

Figure 4. The mechanisms and of electrode operation before and after cycling.

cell made with bare Sn/SnO_2 anode is failed after approximate 30 cycles. Initial discharge capacity of bare Sn/SnO_2 anode is 1100 $mAhg^{-1}$ and capacity fading rate is very fast after 10 cycles. It is believed this capacity decrease is because of Sn-based electrode disintegration caused by a high-volume increase (18). Sn/SnO_2/MWCNT anode showed 1241 $mAhg^{-1}$ initial discharge capacity. The capacity retention is still high as 390 $mAhg^{-1}$ even after 100 cycles electrochemical test.

The mechanisms of electrode operation during lithium insertion and extraction are shown in Figure 4. Furthermore, SEM images of the anodes after electrochemical cycling tests were presented in Figure 4. The large volume variation leads to the pulverization of the bare Sn/SnO_2 anode after cycling. However, Sn/SnO_2/MWCNT anode provided a solution to dimensional instability problems by limiting the changes in volume of electrode. The MWCNT buckypaper acts as both mechanical support and electrical conductor. The buffering effect of Sn/SnO_2/MWCNT nanocomposite gives the battery dimensional stability and can prevent the repeated aggregation and pulverization of the dispersed tin nanoparticles during charging and discharging.

EIS is a useful technique to study the electrode kinetics of anode as well as cathode materials. EIS measurement was carried out to understand the electrode reaction kinetics and the SEI cathodic peak is submerged in the first cycle, which cannot be observed in the CV profiles (19). Presently, we examined the impedance spectra of Sn/SnO_2/MWCNT nanocomposite anode with Li-metal as the counter electrode at various voltages, 1.0 V−2.2 V. Figure 5a and b shows the Nyquist plots (Z' vs. $-Z''$) during the first discharge cycle. The impedance spectra were fitted to an EC, shown in Figure 5c, consisting of resistance (electrolyte, surface film (sf) and charge-transfer (ct)), a Warburg impedance and intercalation capacitances. The fitted values using equivalent electrical circuit are shown in Table 1. The semicircle in the high-frequency region of the Nyquist plot is mainly the contribution of the solid electrolyte interphase (SEI) film on the electrode (19). Based on the EIS measurement, we as certain the potential of SEI film formation,

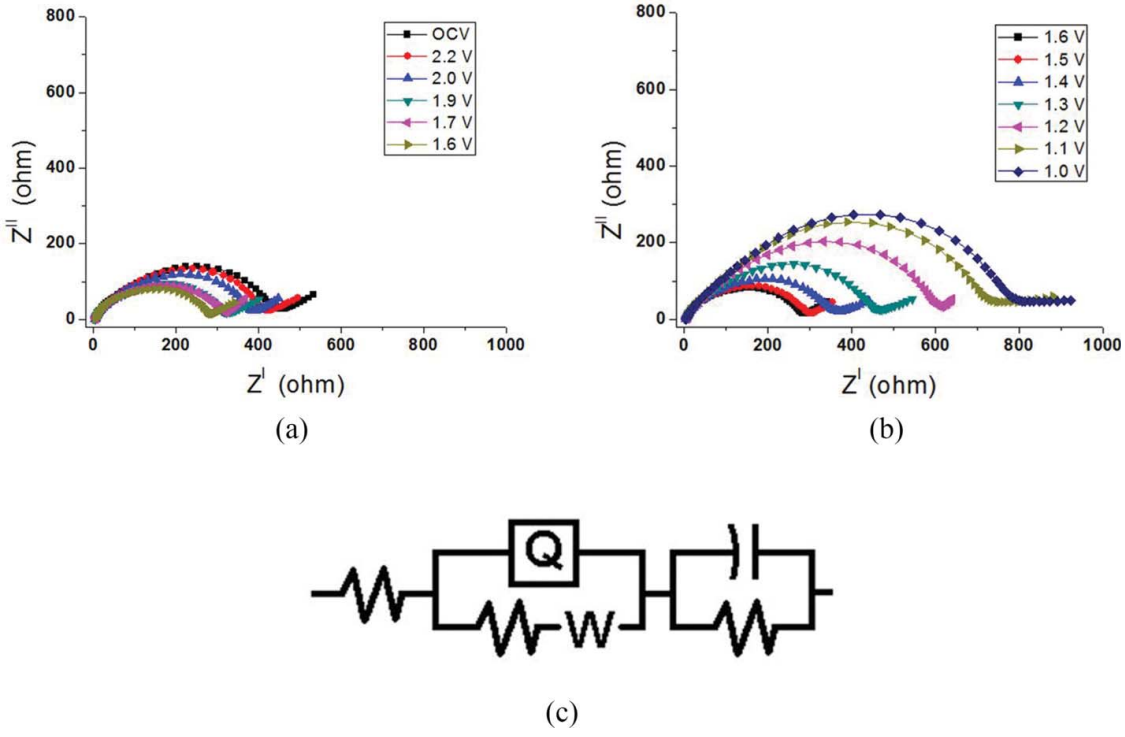

Figure 5. (a) and (b) Family of Nyquist plots for the Sn/SnO_2/MWCNT anode during first discharge (c) equivalent electrical circuit used to fit the data of Figure 5a and b.

Table 1. Impedance parameters of Sn/SnO_2/MWCNT anode during first discharge at various voltages.

Cell voltage	R_e (Ω)	R_{sf} (Ω)	R_{ct} (Ω)
ocv	3.3	41.8	25.1
1.0	4.2	80.8	17.2
1.1	4.0	62.2	18.4
1.2	3.9	59.4	20.4
1.3	3.7	43.8	21.8
1.4	3.5	33.5	24.2
1.5	3.6	30.7	25.1
1.6	3.6	33.5	26.5
1.7	3.5	35.8	28.3
1.8	3.5	27.8	25.3
1.9	3.4	34.7	22.1
2.0	3.2	34.4	20.4
2.1	3.3	39.4	19.1
2.2	3.2	38.3	19.0

and verify the previous conjecture for the SEI cathodic peak in the CV measurements (15).

4. Conclusions

Sn/SnO_2/MWCNT nanocomposite electrode was successfully produced using MWCNT buckypaper as flexible and freestanding by thermal evaporation and subsequent plasma oxidation. Double phase structure was achieved by plasma oxidation. Sn/SnO_2 structure was also deposited MWCNT surfaces creating core-shell structure. Electrochemical performance of Sn/SnO_2/MWCNT nanocomposite electrode was comprised with Sn/SnO_2 thin film onto stainless steel substrates. Sn/SnO_2/MWCNT nanocomposite showed outstanding performance with high capacity and satisfactory cycling stability. Even at 100 cycles, no cell failure was detected all the studied cell assemblies. Extremely high discharge capacity of nanocomposite electrodes makes them good candidates for possible microbattery applications. EIS studies were shown first discharge cycle. Impedance parameters were calculated to fitting an equivalent electrical circuit.

Acknowledgments

The authors would like to acknowledge the financial support of Scientific and Technical Research council of Turkey (TUBITAK) under the contract number 109M464 and Sakarya University, Coordination of Scientific Research Project (BAPK) under the contract number 2010-50-02-017.

References

1. Nitta, N., Wu, F., Lee, J.T., and Yushin, G. (2015) Li-ion battery materials: Present and future. *Mater Today*, 18(5): 252–264.
2. Noerochim, L., Wang, J. Z., Chou, S. L., Wexler, D., and Liu, H. K. (2012) Free-standing single-walled carbon nanotube/SnO_2 anode paper for flexible lithium-ion batteries. *Carbon*, 50(3): 1289–1297.
3. Liu, H., Huang, J., Li, X., Liu, J., Zhang, Y., and Du, K. (2012) Flower-like SnO_2/graphene composite for high-capacity lithium storage. *Appl Surf Sci*, 258(11): 4917–4921.
4. Tocoglu, U., Cevher, O., Guler, M. O., and Akbulut, H. (2014) Coaxial silicon/multi-walled carbon nanotube nanocomposite anodes for long cycle life lithium-ion batteries. *Appl Surf Sci*, 305: 402–411.
5. Tokur, M., Algul, H., Uysal, M., Cetinkaya, T., Alp, A., and Akbulut, H. (2016) Electrolytic coating of Sn nano-rods on nickel foam support for high performance lithium ion battery anodes. *Surf Coat Technol*, 288: 62–68.
6. Guler, M. O., Cetinkaya, T., Tocoglu, U., and Akbulut, H. (2014) Electrochemical performance of MWCNT reinforced ZnO anodes for Li-ion batteries. *Microelectron Eng*, 118: 54–60.
7. Gul, H., Uysal, M., Guler, M. O., Alp, A., and Akbulut H. (2014) Preparation of Sn-Co alloy electrode for lithium ion batteries by pulse electrodeposition. *Int J Hydrogen Enery*, 9: 1–6.
8. Uysal, M., Cetinkaya, T., Kartal, M., Alp, A., and Akbulut, H. (2014) Production of Sn–Cu/MWCNT composite electrodes for Li-ion batteries by using electroless tin coating. *Thin Solid Films*, 572: 216–223.
9. Dong, P. P., Hui, Y., Lang, X., Nan, J. M., and Chen, H.Y. (2015) Facile synthesis cuboid SnO_2 nanoparticles and electrochemical properties as anode of lithium ion battery. *Russ J Electrochem*, 51(8): 712–718.
10. Wu, Z., Li, X., Tai, L., Song, H., Zhang, Y., Yan, B., et al. (2015) Novel synthesis of tin oxide/graphene aerogel nanocomposites as anode materials for lithium ion batteries. *J Alloys Compd*, 646: 1009–1014.
11. Alaf, M., Gultekin, D., and Akbulut, H. (2013) Electrochemical properties of free-standing Sn/SnO_2/multi-walled carbon nano tube anode papers for Li-ion batteries. *Appl Surf Sci*, 285: 244–251.
12. Levi, M. D., Gofer, Y., and Aurbach, D. (2004) Effect of the structure of nonuniform conducting polymer films on their electrochemical impedance response. *Russ J Electrochem*, 40(3): 273–279.
13. Churikov, A. V., Pridatko, K. I., Ivanishchev, A. V, Ivanishcheva, I. A., Gamayunova, I. M., and Zapsis, K. V., et al. (2008) Impedance spectroscopy of lithium–tin film electrodes. *Russ J Electrochem*, 44(5): 594–601.
14. Tocoglu, U., Alaf, M., Cevher, O., Guler, M. O., and Akbulut, H. (2012) The effect of oxidants on the formation of multi-walled carbon nanotube buckypaper. *J Nanosci Nanotechnol*, 12(12): 9169–9174.
15. Alaf, M., and Akbulut, H. (2014) Electrochemical energy storage behavior of Sn/SnO_2 double phase nanocomposite anodes produced on the multiwalled carbon nanotube buckypapers for lithium-ion batteries. *J Power Sources*, 247: 692–702.
16. Alaf, M., Gultekin, D., and Akbulut, H. (2014) Double phase tinoxide/tin/MWCNT nanocomposite negative electrodes for lithium microbatteries. *Microelectron Eng*, 126: 143–147.
17. Zhao, L., and Gao, L. (2004) Coating of multi-walled carbon nanotubes with thick layers of tin (IV) oxide. *Carbon*, 42: 1858–1861.
18. Fu, Y., Ma, R., Shu, Y., Cao, Z., and Ma, X. (2009) Preparation and characterization of SnO_2/carbon nanotube composite for lithium ion battery applications. *Mater Lett*, 63(22): 1946–1948.
19. Zhao, S., Bai, Y., and Zhang, W. (2010) Electrochemical performance of flowerlike $CaSnO_3$ as high capacity anode material for lithium-ion batteries. *Electrochim Acta*, 55(12): 3891–3896.